12th IWSA, Beijing 2006

Fracture-induced seismic anisotropy when shearing is involved in production from fractured reservoirs

N. Barton
Nick Barton & Associates, Oslo, Norway

ABSTRACT

Conducting, 'open' joints, fractures or microcracks parallel to the classic direction $\sigma_{H\,max}$ are commonly referred to in the geophysics literature. They are the focus for most of the shear wave polarization studies, and are often assumed to be stress-aligned microcracks. Nevertheless, measurements in deeper wells reported during the last 10-15 years by Stanford University researchers, do not show conducting joints parallel to the 'classic' direction $\sigma_{H\,max}$. The *non-conducting* fractures in these deep wells are in the directions relative to $\sigma_{H\,max}$ that are normally assumed to be *conducting directions* in geophysics literature. The conducting joints in deep wells are found to be consistently in conjugate directions, bisected by the 'classic' $\sigma_{H\,max}$ direction, so shear stress may therefore be acting to assist in their permeability. Numerous fractured reservoir cases in fact show 20º to 40º rotations of the polarization axes of qS_1 and qS_2, relative to interpreted $\sigma_{H\,max}$ directions, possibly because more than one set of fractures is present, as expected in most rock masses. Shearing induced by reservoir production and compaction, on one or more sets of fractures, is also known to be an important contributor to the maintenance of permeability in the face of increased effective stress. Shearing of conjugate sets of fractures is also considered by the author as a potential source of the temporal rotation of seismic anisotropy and attenuation, as recently recorded in 4D seismic at the Ekofisk and Valhall reservoirs in the North Sea.

1 INTRODUCTION

A standard assumption in the geophysics literature is that shear wave polarization and splitting occurs due to stress-aligned structure. This structure has been considered by many to be stress aligned microcracks, by others with reservoir interests, as a desirable 'open' set of sub-vertical conducting fractures that are also assumed to be parallel or sub-parallel to the maximum horizontal stress.

Although the surface roughness of joints or fractures is known from numerous studies in rock mechanics, to be an important contributor to the stress-dependent hydraulic aperture, e.g. Barton et al. 1985, it is actually difficult to model sufficient hydraulic apertures (e) to satisfy the 'open fractures' concept. The joints or natural fractures may be acted on by an effective normal stress, i.e. $\sigma_{H\ min}$, as high as 25 to 50 MPa. Unless the rock is very strong with high 'joint wall compressive strength (JCS: maximum range of e.g. 10 to 200 MPa), and the joint or fracture surfaces are quite rough, with high 'joint roughness coefficient' (JRC: maximum range of e.g. 0 to 20) the expected 'open' fractures may be hard to justify from a geomechanics viewpoint. However, other potentially 'open' fractures are of course those that are partially 'bridged' by mineral deposition at some time in the geologic past, leaving channels that tend not to be closed by high effective normal stress levels. Various categories of mineralized fractures have been described by Laubach et al., 2002.

The joint index parameters JRC and JCS have been widely used in rock mechanics since they were introduced in 1973, and refined by numerous tests in Barton and Choubey, 1977. They form part of the Barton-Bandis joint constitutive laws linking stress, deformation (closure, or slip-dilation), permeability and jointed-block size. They have been summarized in detail in Barton, 2006. These same index parameters can also be used to demonstrate that there are unlikely to be commercially viable hydrocarbon-bearing fractures or joints with *very low* roughness or JRC values, or with *very low* wall strength or JCS values, as joint closure under stress would preclude both permeability and 'storage', if such was needed due to low-porosity matrix.

An example of joint-closure-permeability and joint-shear-dilation-permeability modelling for the case of weak rock (JCS = 25 MPa) and rather planar joints (JRC = 5) is given in Figure 1. Joint closure illustrated on the left is 'complete', but even small amounts of shear generate sufficient dilation for much improved permeability. In contrast, Figure 2 demonstrates the positive effect of stronger rock (JCS = 50 MPa) and rougher joints (JRC = 10). Reasonable apertures may be maintained in the case of the latter, without the requirement for shear-enhanced permeability.

Barton Bandis Joint Model			NORMAL CLOSURE CALCULATION					
INPUT PARAMETERS		SNORM	CYCLE 1	CYCLE 2	CYCLE 3	CYCLE 4	CYCLE 5	
JRC	5	LOAD	20	20	20	10	0	MPa
JCS	25	UNLOAD	0	0	0	0	0	MPa
SIGMAC	30	APERTURE	0,140	0,030	0,020	0,016	0,015	mm
		KNP	4,60E+03	2,80E+04	4,50E+04	1,40E+04	3,00E+01	
CALCULATED PARAMETERS								
		KNI	4,76	16,42	24,13	29,18	30,42	MPa/mm
	LOAD	VMI	-0,140	-0,030	-0,020	-0,016	-0,015	mm
		AJ	0,210	0,061	0,041	0,034	0,033	
		BJ	1,499	2,030	2,100	2,125	2,130	
	UNLOAD	KNI'	16,42	24,13	29,18	30,42	23,64	MPa/mm

INPUT PARAMETRS			FULL SCALE PARAMETERS		
JRCo	5,00		JRCn	4,26	
JCSo	25,00	MPa	JCSn	19,64	MPa
Lo	0,10	M	DPEAK	2,03	mm
Ln	0,50	M	ROUGH	1,25	
PHIr	27,00	DEG	LFACT	0,01	
SIGMA n	10,00	MPa	PHIr RAD	0,47	Rad
SIGMAC	30,00	MPa	PPEAK	28,25	Degrees
APERTURE	0,000	mm	KS	2,650	MPa/mm

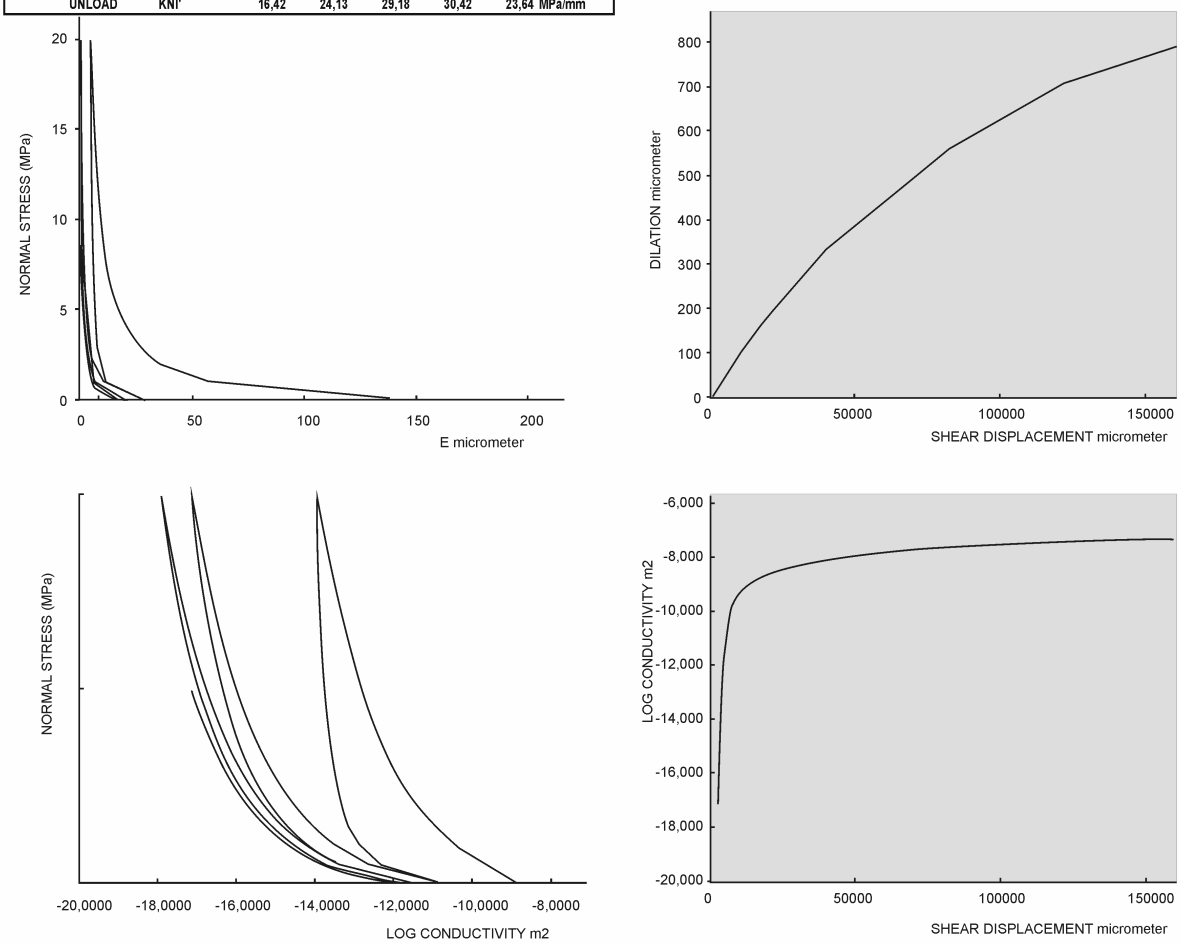

Figure 1. Modelling of stress-closure-permeability, and shear-dilation-permeability, for the case of weaker rock with moderately planar joints. This Barton-Bandis constitutive model is described in Barton, 2006.

Barton Bandis Joint Model			NORMAL CLOSURE CALCULATION					
INPUT PARAMETERS		SNORM	CYCLE 1	CYCLE 2	CYCLE 3	CYCLE 4	CYCLE 5	
JRC	10	LOAD	20	20	20	10	0	MPa
JCS	50	UNLOAD	0	0	0	0	0	MPa
SIGMAC	60	APERTURE	0,280	0,090	0,068	0,059	0,056	mm
CALCULATED PARAMETERS								
LOAD		KNI	13,5	20,17	23,4	25,41	26,33	MPa/mm
		VMI	-0,277	-0,063	-0,039	-0,032	-0,029	mm
UNLOAD		KNI'	16,42	24,13	29,18	30,42	23,64	MPa/mm

INPUT PARAMETRS			FULL SCALE PARAMETERS		
JRCo	10,00		JRCn	7,25	
JCSo	50,00	MPa	JCSn	30,85	MPa
Lo	0,10	M	DPEAK	2,42	mm
Ln	0,50	M			
PHIr	33,00	DEG			
SIGMA n	10,00	MPa			
SIGMAC	60,00	MPa	PPEAK	36,55	Degrees
APERTURE	29,500	μm	KS	3,067	MPa/mm

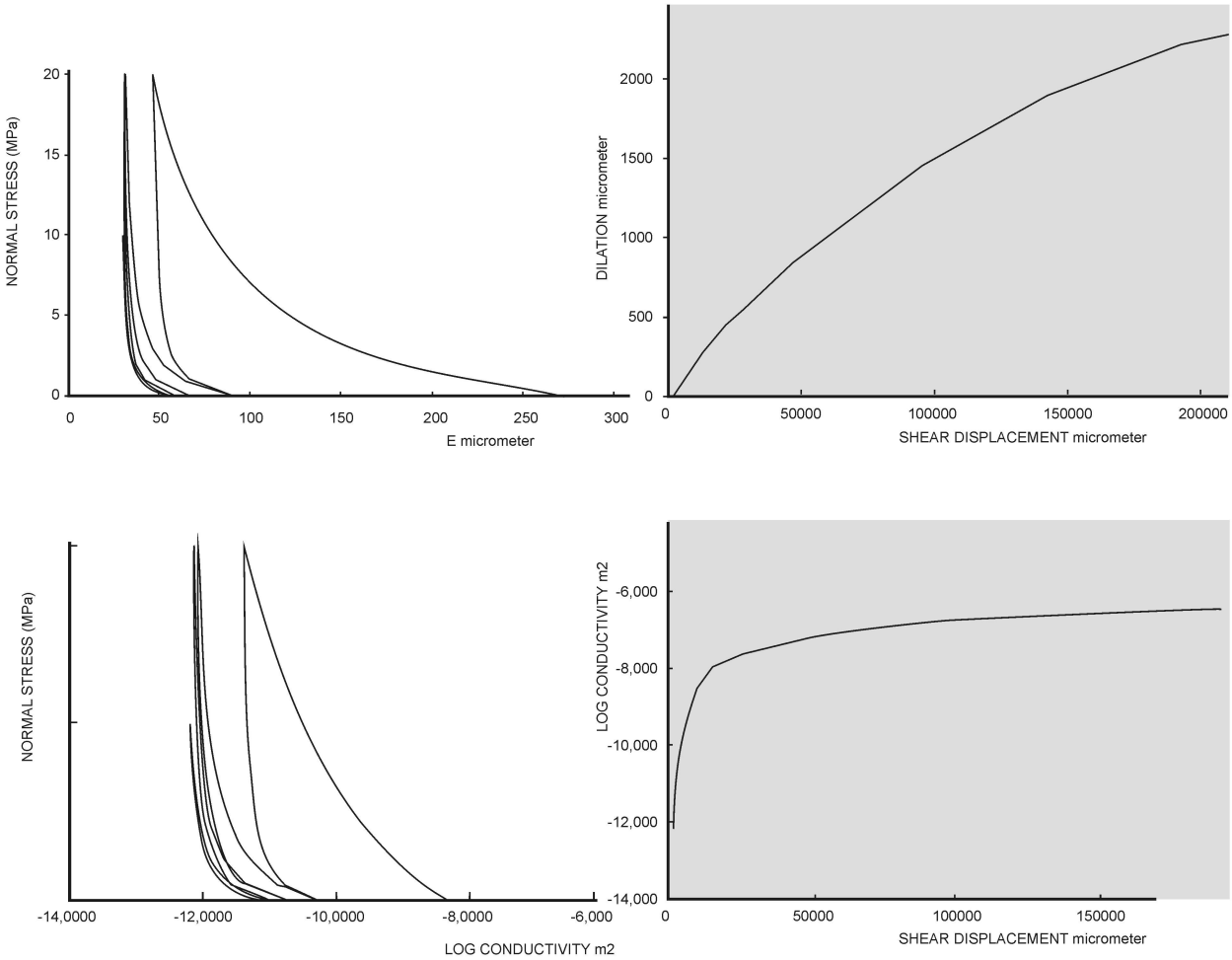

Figure 2. Modelling of stress-closure-permeability, and shear-dilation-permeability, for the case of stronger rock with rougher joints.

2 DEEP WELL MEASUREMENTS OF CONDUCTING FRACTURES

Measurements in deep wells reported by Stanford University researchers (e.g. Zoback and Townend, 2001, Colleen Barton et al 1995), do not show conducting joints parallel to the 'classic' direction $\sigma_{H\ max}$. The conducting joints in deep wells in hard crystalline rocks are found to be consistently in conjugate directions, bisected by the 'classic' $\sigma_{H\ max}$ direction. This

means that shear stresses may therefore be acting to assist in their permeability, as suggested in Figure 3, despite normal effective stresses of 50-75 MPa.

The *non-conducting* fractures in these deep wells are in the directions relative to $\sigma_{H\ max}$ that are normally assumed to be *conducting directions* in geophysics literature, i.e. closed 'only' by a normally directed $\sigma_{H\ min}$, which already may be tens of MPa, unless over-pressured. Mobilized friction coefficients μ of mostly 0.5 to 0.9 have been interpreted in the case of numerous deep wells with such conducting fractures (Townend and Zoback, 2000, Zoback and Townend, 2001), and these have been analysed in terms of non-linear shear strength laws in Barton, 2006.

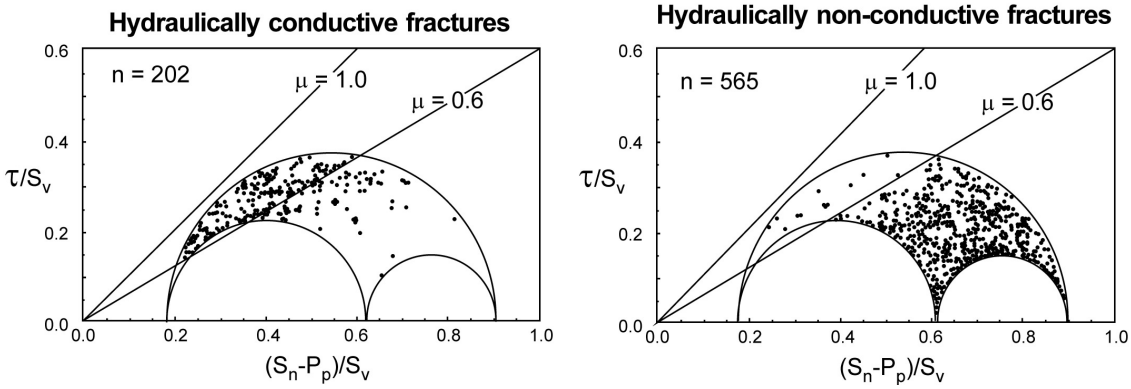

Figure 3. Mohr stress representation of Cajon Pass fractures and their conducting or non-conducting orientations, depending on resisted shear stress. Colleen Barton et al. 1995.

3 ALTERNATIVE MODEL INVOLVING SHEAR

In view of the above modelling result with JRC and JCS, and in view of the above deep-well findings, this paper examines alternative interpretations of shear-wave polarization directions, specifically the contribution of two, maybe unequal joint or fracture sets, bisected by the major stress. It is further assumed that the two sets may have different compliances, and that they possibly will have pre-peak-shear-strength dilation contributions to their enhanced permeability.

The coupled 'geomechanics-geophysics' alternative model for explaining 'open fractures' even at depth, is illustrated in exaggerated format, in Figure 4. Such a model, expanded to

show two sets, would give a shear wave polarization direction formed by the resultant of the compliances of each set which might approximate the bisecting $\sigma_{H\ max}$ direction, depending also on relative magnitudes of continuity and spacing for the two sets. Sayers, 2002 described a related case of shear-wave splitting when the incident waves were no longer parallel to the vertical fracturing, due to the presence of a conjugate pair of fracture sets.

This alternative seems to be well supported by deep well data, and by water-flood principal permeability directions, which range, significantly, on both sides of the $\sigma_{H\ max}$ direction, according to data from numerous fractured reservoirs (Heffer, 2002, and Tingay et al. 2005). As we shall see, several reservoir cases reviewed in Barton 2006, in fact show 20º to 30º rotations of the polarization axes of qS_1 and qS_2, relative to the borehole break-out interpreted $\sigma_{H\ max}$ direction. This may be due to the component contributions from two sets.

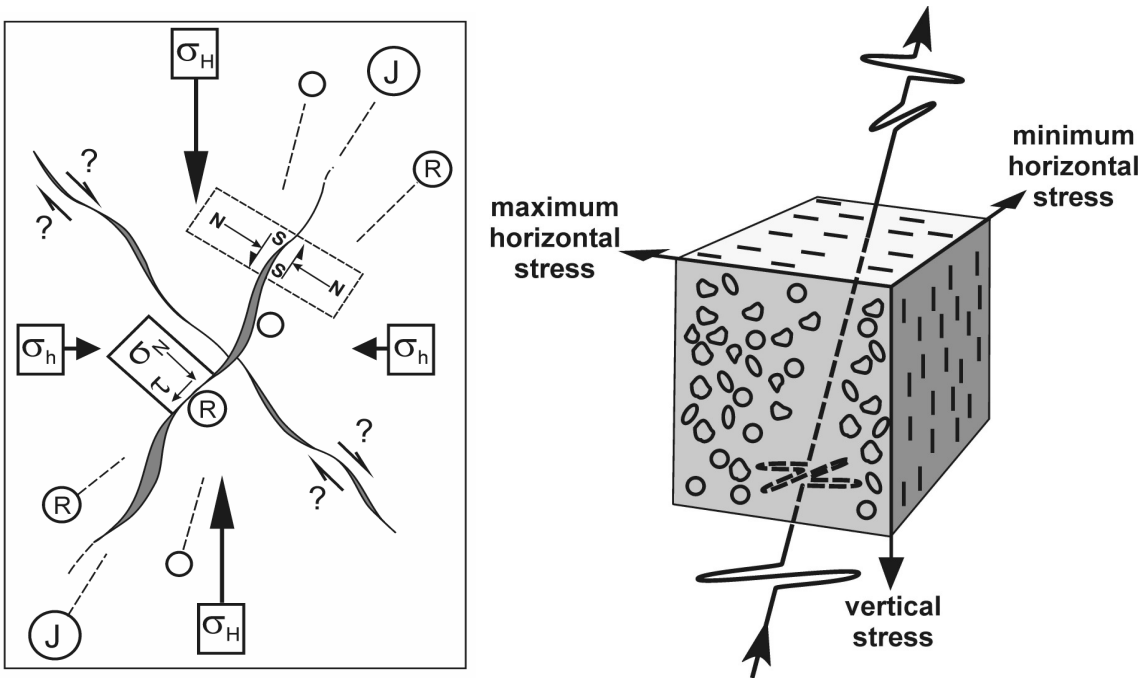

Figure 4. A geomechanics model (left) that is capable of matching deep-well measurements of permeable fracture directions, and that could also cause shear wave polarization sub-parallel-to-the-$\sigma_{H\ max}$ direction, as frequently observed (e.g. Barton, 2006). In the case of polarization components from two sets, the classic microcrack or crack model of Crampin and Lovell, 1991 (right) would need to be extended beyond the single set of stress-aligned cracks.

4 EVIDENCE FOR POLARIZED SHEAR WAVES DEVIATED FROM $\sigma_{H\ MAX}$

Offshore 3D seismic surveys, using compressional P-wave sources converted to PS at the sea-floor, thereafter analysed as S-waves , or use of P-wave or direct S-waves (SS) generated on land, in walk-away, multi-azimuth VSP, are basic geometries for shear-wave polarization and anisotropy investigations above fractured reservoirs. The conventional belief is that the split shear waves S1 (or qS_1) and S2 (or qS_2) result from major principal stress-aligned dominant fracturing or micro-fracturing. A conventional interpretation is shown in Figure 5, from Stenin et al. 2002.

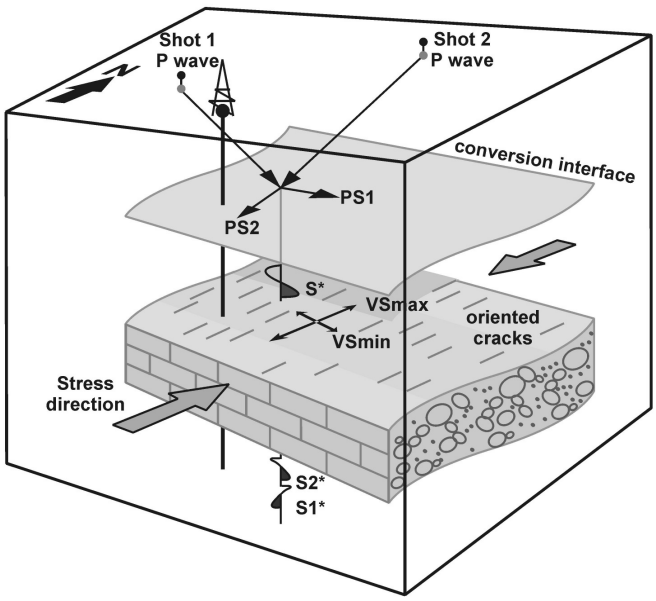

Figure 5. Far-offset VSP, showing P-wave conversion to PS waves at an interface, with subsequent polarization to fast S1 and slow S2 shear-waves, due to assumed stress- aligned structure. Stenin et al. 2002.

A supplementary interpretation, that perhaps two or more sets of unequal conjugate fractures could be responsible for shear-wave polarization, and indeed responsible for efficient production from fractured reservoirs, can be suspected from water flood interpretation given by Heffer, 2002, shown in Figure 6. At the top is the conventional expectation of open fractures parallel to S_{max} (or σ_{Hmax}). Below is the data base, showing in fact that a considerable number of fracture sets are bisected by the principal stress, and may have suffered some permeability-enhancing pre-peak shear displacement, which may also cause a *deviation* of both permeability and shear-wave polarization from the classic $\sigma_{H\,max}$ direction, if one set is dominant.

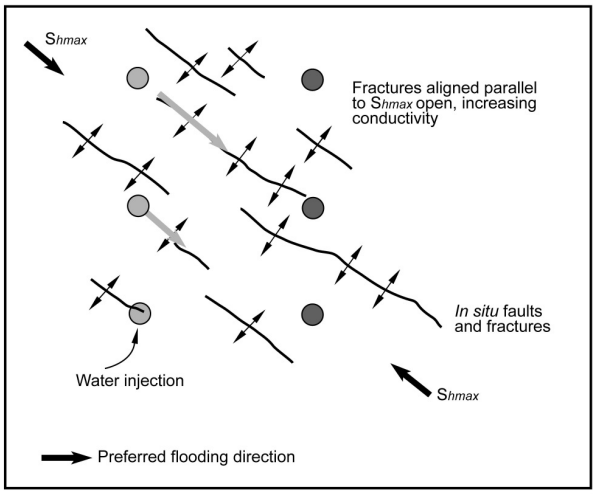

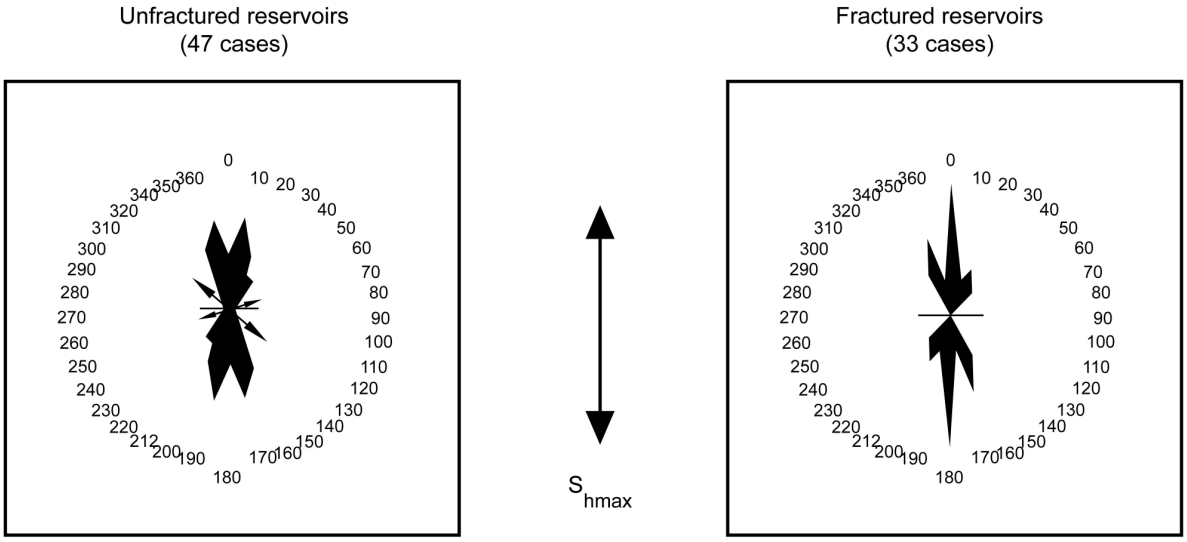

Figure 6. a) Standard interpretation of water-flood flow-directionality trends in fractured reservoirs, and b) rosette data for fractured and 'unfractured' reservoirs from Heffer, 2002 suggest contributions to flow from 'conjugate' sets.

Civil engineering near-surface evidence for approximate 'line-up' of dominant structure, major horizontal stress, permeability and maximum P-wave velocity, can be deduced from the literature (Barton, 2006). This near-surface experience has also been repeated in near-surface oil-well investigations, as suggested from the upper 30 m of data from the Conoco borehole experiments reproduced in part in Figure 7.

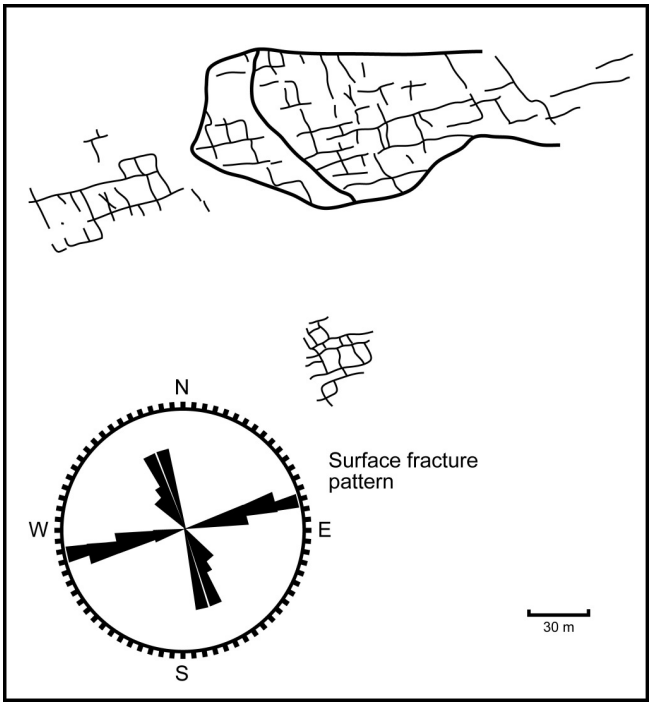

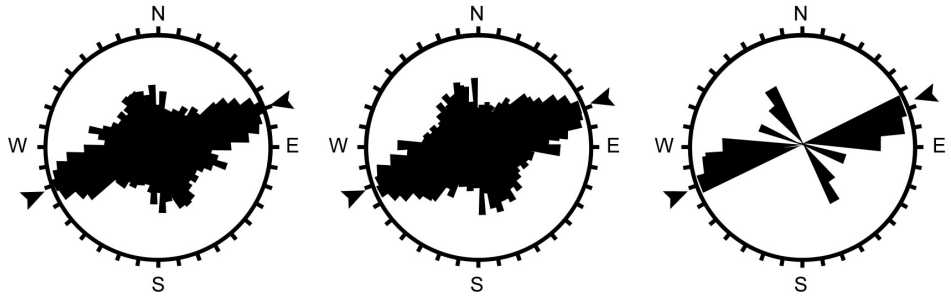

Figure 7 a) Near-surface, dominant fracture sets at the Conoco borehole site. Because of the shallow location, b) microcracking, dominant polarization of shear-waves, and the inferred jointing tend to be // to $\sigma_{H\,max}$ *(Liu et al. 1993).*

However, at greater depth in the same well, there was *deviation* of observed fracturing azimuth from the shear-wave polarization *resultant* azimuth. This deviation is shown in Figure 8 from Queen and Rizer, 1990. This seems to be one of many indications that shear waves may split in response to the relative strength of multiple sets of fractures or joints.

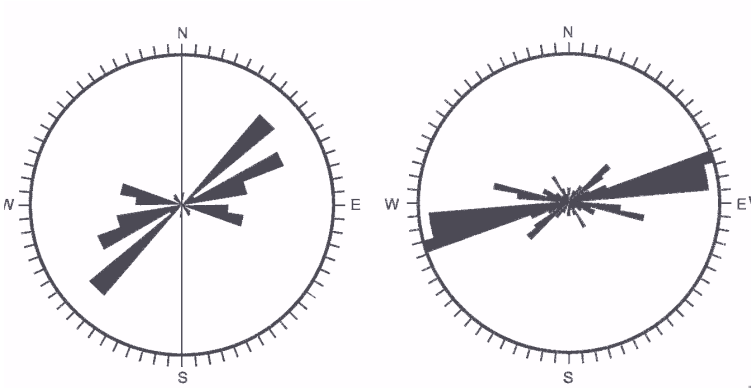

Figure 8. Conoco Borehole Test Facility analysis of fracturing from 150 to 850 m depth. Left: accumulative length of BHTV- and oriented core-identified fracturing. Right: combined azimuths from nine-component VSP shear-wave polarization, from all levels. Queen and Rizer, 1990.

At the UK offshore Claire Field, Smith and McGarrity, 2001 described multi-azimuth walk-away (i.e. float-away) VSP. Down-hole triaxial accelerometer arrays were used both in the fractured reservoir (1850-1905 m) and in the over-burden (1486-1535 m). The authors pointed out that P-waves travelling obliquely can be influenced by the 'shear properties of the rock', presumably meaning the shear compliance of the fractures. The authors also referred to the normal dominance of one fracture set with an orthogonal sub-set, and referred to the variation of *fracture density* in this unequal two-set system, as the reason for variations in the degree of seismic anisotropy. One could take this a stage further and suggest that *if* the major stress was bisecting these two sets, and *if* shear stress was involved, production could also cause temporal rotation of the anisotropy axes, and even of the attenuation axes.

A later study by Maultzsch et al., 2005, addressed the question of *attenuation anisotropy* at this field. They also used the earlier multi-azimuth walk-away VSP results, and demonstrated that the fractured, oil-saturated reservoir also showed a consistent azimuthal variation in attenuation. They analysed attenuation as a function of azimuth for each offset, both in the reservoir and in the overburden, utilising the two tool settings. In the reservoir, minimum attenuation lay between N70ºE and N100ºE, but at the shallower receiver setting in the overburden, the minimum attenuation was scattered between wider azimuths.

Rose diagrams of all the fractures and of the open conducting fractures, from others' logging of cores and borehole images are reproduced in Figure 9. Maultzsch et al., 2005, also provide in Figure 9c their measured azimuth of minimum attenuation, which is *actually some 20º*

oblique to the open fractures. The major horizontal stress from Smith and McGarrity, 2001, is close to parallel to the open fractures, yet the minimum attenuation was 20º different.

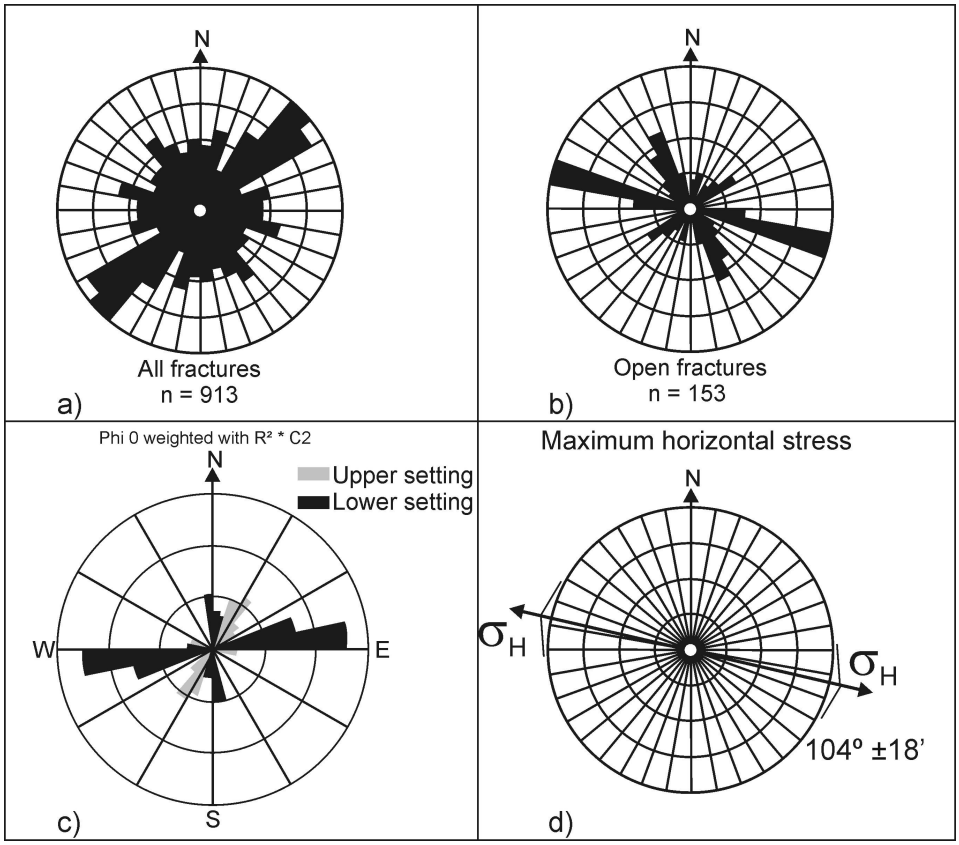

Figure 9. Multi-azimuth walk-away VSP at the Claire Field: Despite the consistency of 'open' fractures and the interpreted major horizontal stress, the minimum attenuation axes(c) for the reservoir (black) are not consistent with these two directions. Deviation of the attenuation azimuth in 4D interrogation of some recently instrumented reservoirs, may be further evidence that shear stress is involved in other cases too. Smith and McGarrity, 2001, Maultzsch et al. 2005.

The authors Pérez et al., 1999 compared independently acquired 3D azimuthal AVO results with shear-wave related studies, using C-wave (P to S converted waves), and the shear-wave splitting mechanism. They acquired data from three intersecting 10 km long, three-component seismic lines, with three different azimuths. The three lines intersected at one of the wells, where there were results of FMS (formation micro-scanner) and caliper logs for estimating both the dominant fracture strike and the direction of $\sigma_{H\ max.}$ The latter was oriented NW-SE,

and the authors assumed that the fracture set in approximately this direction (one of several sets), would be the one most likely to be 'open', and therefore most detectable.

In this study the far offset extended to 3600 m, a bit more than the depth of the target zone: a 35 m thick fractured limestone at approximately 3000 m depth. This had a P-wave velocity of only 3513 m/s, and an S-wave velocity of 1890 m/s, with a density of 2.5 gm/cm^3. In other words it would seem to have been extremely well fractured or over-pressured, since the porosity does not seem to be high, judging by this density.

Figure 10 shows the results of one of the three fracture direction analyses which were described by Pérez et al., 1999. This is from the converted (C) wave P-S analysis, using the shear wave splitting and polarization analysis. The deviation from the $\sigma_{H\ max}$ direction is quite clear. A similar fracture orientation plot was derived from the 3D azimuthal AVO analysis. The authors estimated that the azimuth of the *maximum AVO gradient* was 56º, based on a formula for calculating the reflection coefficients in TIH media. Since this is assumed to be perpendicular to fracture orientation, the fracture azimuth estimate was 146º, which was shown to be as much as *36º* from the interpreted $\sigma_{H\ max}$ direction.

One may reasonably speculate that these significant deviations are due to the presence of a dominant fracture set, together with a secondary set, with the two sets *bisected* by $\sigma_{H\ max}$. Whether the dominant 'open' set could have permeability enhanced by pre-peak shearing (exaggerated in Figure 4a) will remain for further speculation. In this connection, note the evidence for shearing in conjugate sets of fractures in chalk, described later in this paper.

Despite the growing interest in fractured reservoirs, seemingly worldwide, the exploratory wells are nearly always vertical and the target structures often vertical or sub-vertical as well. As a consequence, cores and well-logs often give little or no useful information about the fractures. A fortunate exception is the conjugate fracturing found in anticlinal structures, where samples of both the oppositely-dipping joint or fracture sets can hardly be avoided, as we shall see shortly.

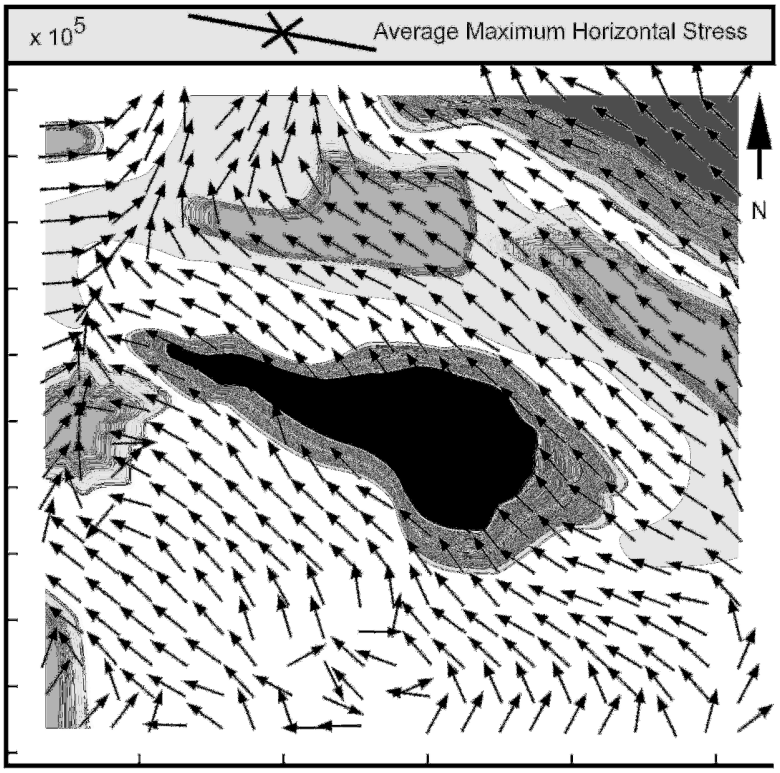

Figure 10. Fractured limestone reservoir at 3 km depth. Converted P-S shear-wave analysis of dominant fracture (or fracture-component ?) directions. Pérez et al. 1999.

Laubach et al. 2000 referred to the use of *sidewall cores* to help pin-point zones that probably have high fracture intensity; not by reaching out to the poorly sampled fractures, but by using *microfracture* and *diagenesis* data to infer the presence of the macro-fractures. Figure 11 shows a comparison of the very consistent microfracture strikes (nearly EW), compared with the broader but consistent orientations of *microfractures*, each data set from the same East Texas well and from the same formation.

One may reasonably speculate that the orientation of the maximum horizontal stress corresponds to that of the microcracks. That being so, the 'symmetric' range of strikes for the macro-fractures means they are conjugate sets and could possibly also be fracture sets under some shear stress, perhaps with extra good conductivity as a result. In fact according to the deep well data cited earlier, they would *need* to be under shear stress, unless the limestone was sufficiently strong, the roughness of the fractures significant, or that the fractures had mineral bridging from an earlier, incomplete mineralization process.

At the recent 12th IWSA in Beijing, numerous examples were presented of fast shear-wave rosettes from earthquake studies in the Fujian district of China (Wu et al., 2006), and from the Beijing capital area (Gao et al., 2006). The rosettes actually resemble the symmetries seen in structural geology joint set rosettes. The same has been seen in the Iceland data published numerous times by Crampin and his co-authors, but interpreted as stress-aligned microcracks. As shown by Boness and Zoback, 2007, shear-wave anisotropy may be caused by preferential closure of macro-fracture sets that are not aligned with $\sigma_{H\ max}$, and of course by the potential 'openness' of the set that is stress aligned. There seems little good reason to always assume that microcracks are involved, when there is such a lot of tectonic structure (joint or fracture sets) that may be either stress aligned, or possibly bisected by $\sigma_{H\ max}$ if still permeable at greater depth.

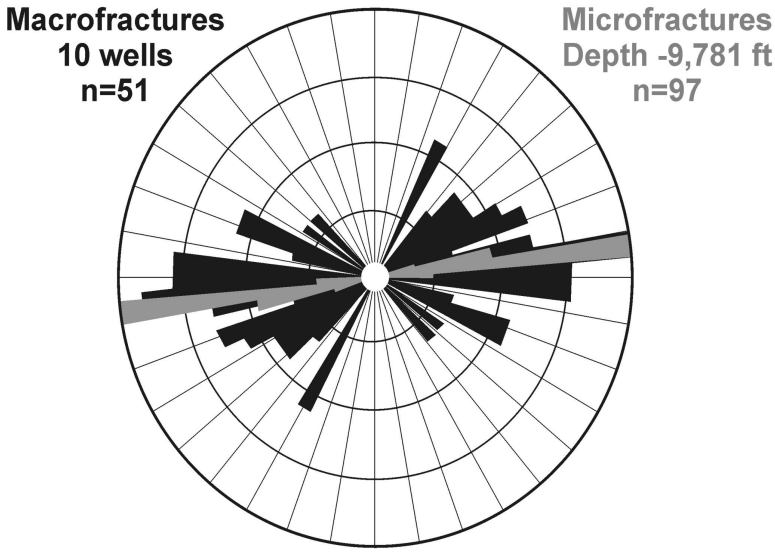

Figure 11. East Texas well data for microcracks and fracture sets in the same formation. Since it may be reasonable to assume that the microcracks are sub – parallel to σ_{Hmax} then it can be assumed that the (conjugate?) fracture sets are roughly bisected by σ_{Hmax}. This may mean that they are also subject to shear stress. (Laubach et al. 2000).

5 OFF-VERTICAL DIPPING FRACTURE SETS

Sayers, 2002 specifically addressed the problem of vertical shear wave propagation in jointed media with *off-vertical dips*, using the example of two conjugate sets with oppositely oriented dip angles, as depicted in Figure 12. Unlike vertical wave propagation through vertical joints, with dependence of shear-wave splitting on only the shear compliances, the shear wave components qS_1 and qS_2 depend here on both the shear *and* normal compliances, since the incident angles are no longer parallel to the joint planes.

As normal compliance is *reduced* (i.e. stiffened) by fluids of non-zero bulk modulus, gas and oil should be distinguishable by respectively greater and less shear wave anisotropy, as the stiffening effect of the oil makes the fracture normal stiffness less contrasted to the background medium (Van der Kolk et al., 2001). For dipping joints or fractures, there proves to be a significant *decrease* in shear wave anisotropy if the fluid has a higher bulk modulus, making the normal *stiffness* of the fractures greater. The average of the two shear wave velocities is therefore also increased.

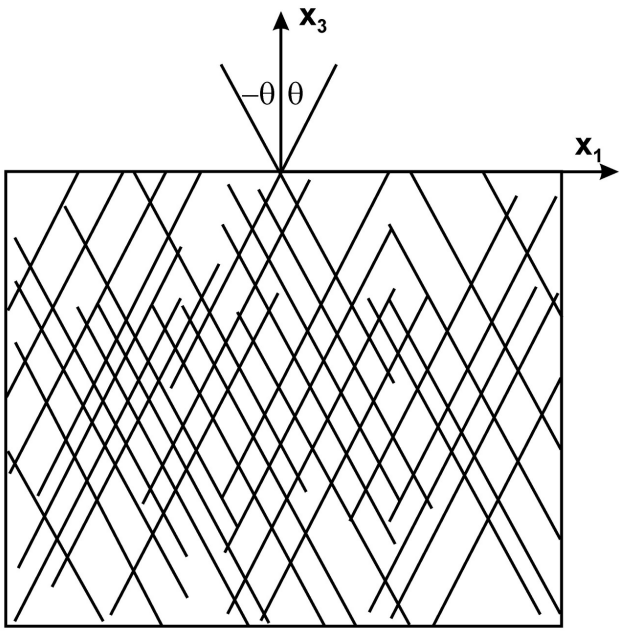

Figure 12. Investigation of shear-wave polarization when incident waves are no longer parallel to vertical fracturing. Sayers, 2000.

Bakulin et al., 2001, also pointed out that both geophysical and geological data acquired over naturally jointed reservoirs often revealed the presence of *multiple* sub-vertical fracture sets, which made the effective medium *monoclinic.* They developed a model for handling two sets of *unequal*, and non-orthogonal vertical joint sets, which yielded the azimuths and compliances of both sets of joints, as well as the P- and S-wave velocities of the assumed isotropic background medium.

6 SHEARING IN A FRACTURED CHALK RESERVOIR

Carbonate or chalk reservoirs of high porosity, and therefore rather low strength, with steeply dipping, as opposed to flat-lying jointing, can apparently continue to be successful oil producers despite strong compaction, because of a remarkable joint shearing mechanism.

Down-dip shearing can occur despite the one-dimensional (vertical) strain boundary conditions that apply during the production-induced compaction of a large tabular reservoir. Matrix shrinkage under an increasingly large increase of effective stress, actually 'makes space' for down-dip shearing of the fractures. This helps to maintain joint aperture due to shear-induced dilation, and apparently may even provide a pseudo-confinement effect (increased k_o: the ratio of horizontal to vertical stress), which surprisingly, could actually make the jointed reservoir somewhat stiffer (in a vertical direction), than the *unjointed* rock (Barton et al., 1986).

Phillips Petroleum geologist's core logging interpretation (H. Farrell, pers. comm.. 1985), of *conjugate* steeply-dipping jointing in the porous, highly productive sections of the 3 km deep Ekofisk reservoir, indicated about 10 to 12 dominant (perhaps > 1 m long) set #1 joints crossing a '1 m window', with oppositely dipping set #2 joints showing about 4 to 6 shorter joints (perhaps 30-50 cm long) in this same 'volume'. These are shown in Figure 13 in an idealized form with constant dip within each set. This of course is a simplification of reality, as we also saw in Figure 12.

The assumed jointing in Figure13 can be shown to represent an accumulated (two-set) *crack (or fracture) density* ($\varepsilon = N.\ r^3/V$) as high as 1.4, which is much higher than the more limited range often referred to in geophysics literature (Barton, 2006).

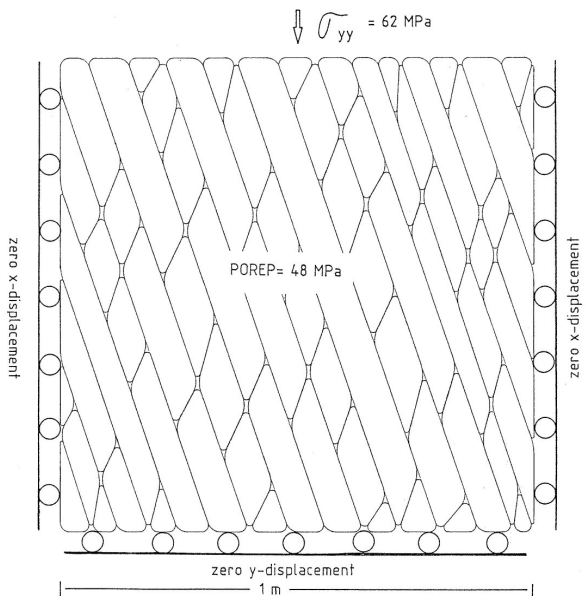

Figure 13 An idealized joint model for 1D compaction modelling, based on the geological description of conjugate jointing in porous Ekofisk chalk. Barton et al. 1986, 1988.

When fracture densities are as high as 1 to 2, as in such well-jointed, domal chalk reservoirs, dimming of the amplitudes of the slow shear-wave, due to greater attenuation caused by lower seismic Q tend to correlate with the most productive parts of the reservoir, as also experienced where the measurable shear-wave anisotropy is greatest. The down-dip shear mechanism may help to maintain apertures (and lower seismic Q), despite high effective stresses in the presence of this weaker, high porosity rock.

If the crack or fracture density is contributed to by two sets of oppositely dipping conjugate fractures, one can expect shear *and* normal compliance contributions from both sets to the slowness of the slow shear-wave, which may be < 2 km/s. The response is strongest when fractures are gas filled, as gas does not stiffen the normal compliance. Attenuation anisotropy should be enhanced in the case of oil-filled fractures, due to the greater contrast of their normal and shear compliances.

The rock mass depicted in 2D in both Figures 13 and 14, tolerated an original *vertical effective stress* of the order of $\sigma_v' \approx 62\text{-}48 = 14$ MPa, with a lower horizontal effective stress. During the first 20 years of production this vertical effective stress had built up to about 38 MPa, due to the 20-24 MPa pore pressure reduction caused by production prior to large-scale water-flooding. This initially unsuccessful attempt to control compaction was followed by 6 m jack-up of all platforms, and final relocation of central platforms, due to the risk of platform damage from large storm waves (up to 30 m), in the increasing depth of sea.

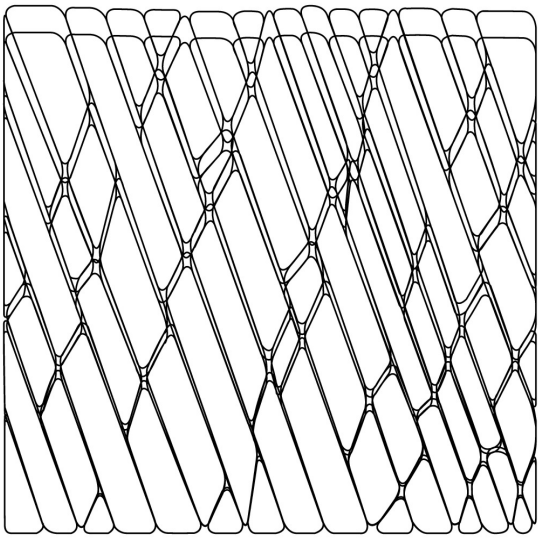

Figure 14. UDEC-BB model of 1D compaction of the porous, conjugately jointed chalk, performed by the NGI team.Barton et al. 1986. The deformation of a 40% porosity chalk is shown, undistorted.

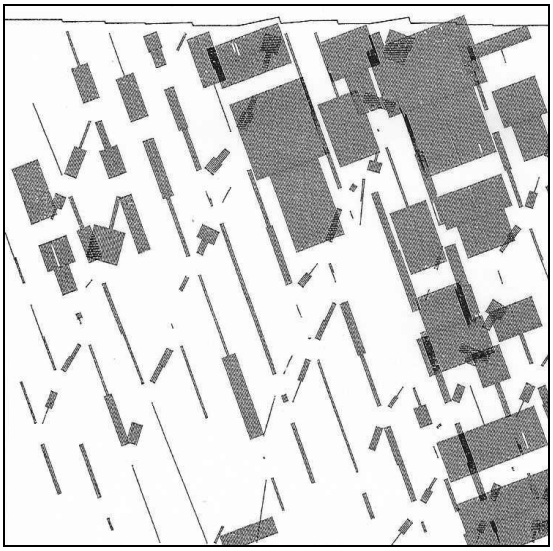

Figure 15 Joint shearing, depicted by the relative size of the symmetric 'flags', was of the order of 4 mm (max.) and 0.4 mm (mean), for the case of the 40% porosity chalk. This was enough to help maintain permeability. Barton et al. 1986.

It may be noted from Figure 15 that the dominance of the 'right-dipping' fracture set also causes unequal magnitudes of shearing, and logically this would bias eventual shear wave polarization in relation to the secondary set. Unequal amounts of pre-peak (even post-peak) shear on fracture sets with different strike could also explain temporal rotation of attenuation axes in 4D monitoring, such as in the Cornwall Hot Dry Rock project in the 1980's (see Crampin and Booth, 1989 and an alternative interpretation in Barton, 1986,), and in the Ekofisk and Valhall chalk reservoirs in this century (various references, see Barton, 2006).

When the Ekofisk fractures were discretely modelled (as in Figures 14 and 15), the pore pressure reduction (in 1985) was limited to 20 MPa. Significantly, in view of the fact that this numerical-model evidence for shearing was not at first believed outside NGI, Albright et al., 1994 mention Ekofisk exhibiting *'shear fracture micro-seismicity, possibly indicating that subsidence is caused by a combination of pore collapse and shear sliding'*. They state that subsidence surpassed early model estimates based on pore collapse, indicating that there were other mechanisms at work. By implication shearing was also occurring at fault scale.

The operator Phillips' core-logging geologists reportedly detected *slickensides* on conjugate joint or fracture sets, when drilling new holes during the 1980's pressure maintenance, using

equilibrated sea-water injection. Slickensides had reportedly *not been detected* in earlier exploration of the Ekofisk field in the late 1960s, where production started in 1971.

The most porous chalk that was first modelled by the NGI team in 1985 (n = 40%), with an assumed axial modulus of only 0.33 GPa, showed maximum shearing of 3.9 mm, with an average of approximately 0.39 mm for all the joints, as in Figure 15. Later modelling by Gutierrez, with a higher pore pressure reduction of 24 MPa, showed up to 10 mm maximum joint shear. Presumably such deforming features would be seismically visible in practice (i.e. a strong source of shear wave splitting), just as the reproduced direct shear tests on rough fractures (Barton, 1973) shown in Figure 16 are 'visible', due to the 'free' dilation that has occurred, due in this case to a constant normal stress application during direct shear testing.

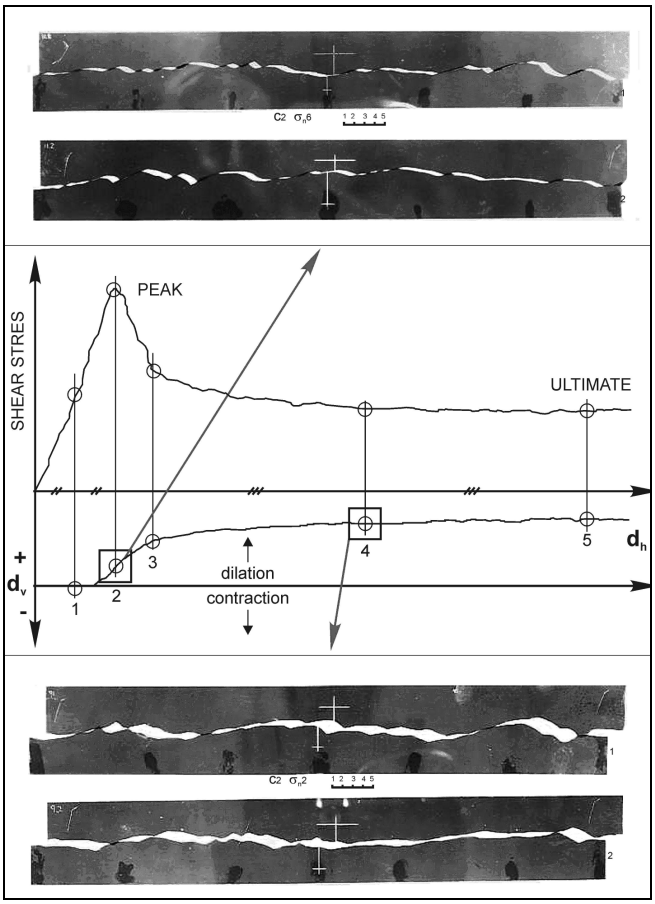

Figure 16. Re-constructed direct shear tests on 10 m long simulated tension fractures, Barton 1973. Although exaggerated in roughness due to tensile origin, and with dilation exaggerated due to constant normal stress, and with gouge not shown (see over-lapped asperities where gouge would result), these physical models help with visualization of a more subtle process that is initiated by shear stress application in the crust. In addition to the beginnings of dilation, there is opposite rotation of 'open' and 'rock-to-rock' contacting areas, when fractures are non-planar, as detailed in Figure 4a. Top: high normal stress and pre-peak. Bottom: low normal stress and post-peak.

7 OVERBURDEN STRETCH AND POLARIZATION

Barkved et al., 2004 referred to the world's first time-lapse, marine, multicomponent (3D/4C) survey, as that performed in September 2002 at the Ekofisk jointed-chalk reservoir in the North Sea. This baseline was subsequently compared with a monitoring survey acquired in December 2003, and of course subsequently this has been repeated. In each case, seabed cables were used to acquire data with a wide range of azimuths. With 'only' about 3×10^8 m^3 of oil out of a total of about 1.1×10^9 m^3 produced by 2003, and production expected to 2050, it is clear that the 'belated' shear-wave technology still has an important role to play also at Ekofisk. Even this first limited time-lapse of 15 months indicated some small changes in the *direction* of the fast shear wave, and in the difference between fast and slow shear velocities. The differences were not consistent across the field.

According to Barkved et al., 2004 the reasons for the small changes detected by the S-waves 'had yet to be understood'. As already noted, the small-scale joint-shearing mechanism identified in distinct element (UDEC-BB) studies for the Norwegian Petroleum Directorate (Barton et al., 1986), that was discussed earlier, was later 'confirmed' by slickensided conjugate joint faces, in core recovered from subsequent wells (post 1985) for water-flooding and production.

According to Phillips Petroleum Co. geologists this slickensiding had not previously been noted, and nor was it noted in the older jointed cores made available to NGI for laboratory direct shear and coupled shear-flow-temperature (CSFT) tests. The shear mechanism may seem surprising in view of the 1D-strain ('roller-boundaries') boundary condition, since a 9 × 14 km reservoir of 300 m thickness can hardly expand laterally during compaction: this occurs more in the stretching, subsiding, overburden as 'seen' by shallow shear-wave splitting at Valhall, to be reviewed shortly.

A *possible* explanation for the small changes of polarization direction and of shear-wave anisotropy at Ekofisk, can perhaps be found in this conjugate (or single) shear mechanism, that was also illustrated in Figure 4a. This mechanism could also be a possible explanation of a larger polarization rotation at the Cornwall hot dry rock geothermal project noted in the 1980's. (Crampin and Booth, 1989). With potential 'opposite-rotation' of fluid lenses and

rock-to-rock contact areas seen in Figure 4a, there could be subtle domination of effects from the primary relative to the secondary conjugate joint set. If the 'O-R' mechanism seen in Figure 4a can be detected by shear waves, *and if the strike of the two conjugate sets is not equally oriented*, then a small rotation of anisotropy axes could be explained.

Variation about the Ekofisk field, with 'radially' trending jointing and rotating principal stress, would easily explain variation of such trends. Others might quote EDA-(micro)-cracks and stress rotation as the possible cause. More subtle structural mechanisms may be at work, and additional complications in the neighbourhood of fault zones are almost inevitable.

At the Valhall Field, quite close to Ekofisk, BP installed a *permanent* seabed cable array, covering 45 km^2 area, to monitor changes using regularly repeated 3D multi-component seismic surveys, to help determine the best reservoir drainage strategy. Olofsson and Kommedal, 2002 presented the first results of shear-wave splitting in the *shallow* overburden, indicating a remarkable, and very convincing match to the assumed 'stretch' of sub-vertical jointing caused by subsidence. Figure 17 shows the result of their shallow overburden shear-wave polarization, with lines showing the qS_1 direction, with their *length* corresponding to the qS_2 time delay or 'lag'.

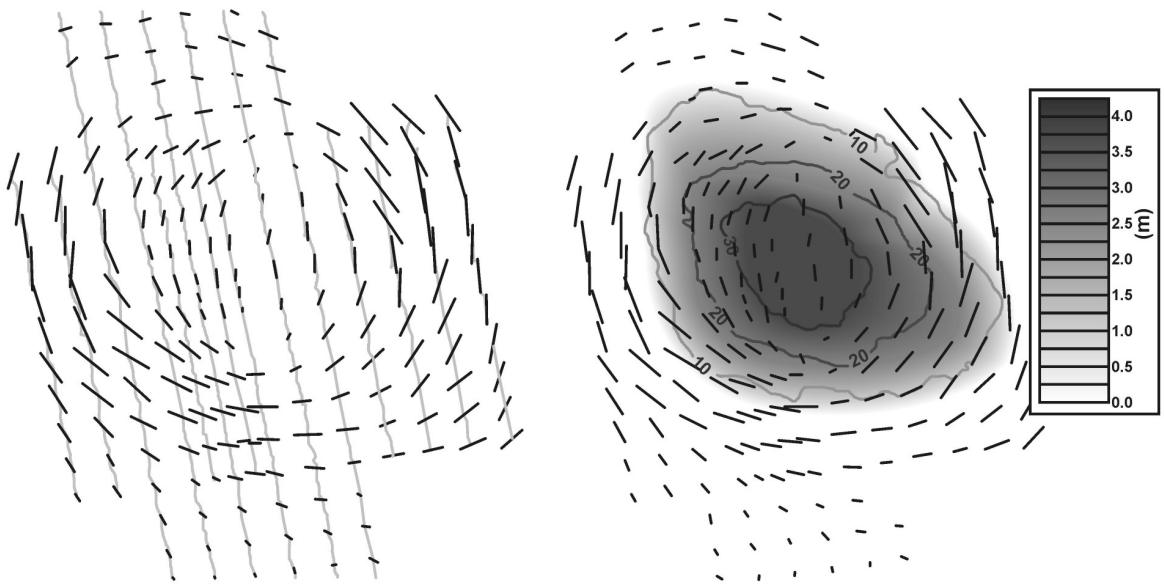

Figure 17. Shear-wave splitting and polarization results for the shallow overburden above the compacting Valhall reservoir. Lines show the qS_1 direction, with their length corresponding to the qS_1 - qS2 time delay or 'lag'. Olofsson and Kommedal, 2002, also Gaiser and Van Dok, 2003 and Barkved et al., 2004. The 'rotation' may correspond to the relative 'visibility' of sub-vertical (bedding-limited?) joints caused by 'stretch' in all directions.

Barkved et al., 2004 also commented on the above near-surface Valhall result, and stated the following: 'The actual mechanism causing the shallow shear-wave splitting is not known. Azimuthal anisotropy is usually associated with fracturing, stress or lithology. In this case the amount of anisotropy is small at the centre of the field, where the subsidence is largest, but the anisotropy is large on the flanks and small again farther from the centre. This strongly points to shear-wave splitting being sensitive to changes in stress or strain.'

The various authors have not apparently focussed on *intra-bed* jointing as the likely source of the partial 'squareness' of some of the strongest anisotropy (i.e. the 'NNE-trending' and longest lines). The depth giving this possible dominant 'imprint' to the polarization and velocity anisotropy is of course not known. Large-scale (axisymmetric, 10 km radius) distinct element modelling of the *Ekofisk* overburden response to modelled compaction, using numerous coarsely 'bedded-jointed-and-faulted (2D) UDEC models (Barton et al., 1986, 1988), showed distinct 'joint' opening and some 'bedding' shear in the overburden, due to the stretch caused by the subsidence. The modelled shearing is shown in Figure 18. These effects worsened with increased compaction profiles, the subsidence/compaction S/C ratio exceeding 0.85 as compaction approached 10 m. Naturally, the stretch is strongest where bending of the strata is largest, and implicitly would show a good match to the consistent Figure 17 shear-wave responses.

A 3D version of such discontinuum modelling (with the 3DEC code, also developed by Cundall), would obviously have shown similar reactions from other perhaps perpendicular 'joint' sets. This 'joint' opening occurred most strongly where bending was strongest, and *least* both centrally and further out beyond the flanks. It is therefore suspected that the 'stress or strain' referred to by Barkved et al., 2004 could rather be termed intra-bed *joint-opening effects,* since the strength and location of these phenomena are likely to match the subsidence-bowl shape at Valhall. Where the polarization is 'diagonal', (i.e. 'NE-SW' or 'NW-SE' relative to the 'N-S' page), presumably the components to polarization (i.e. joint compliance) from both sets could be operating.

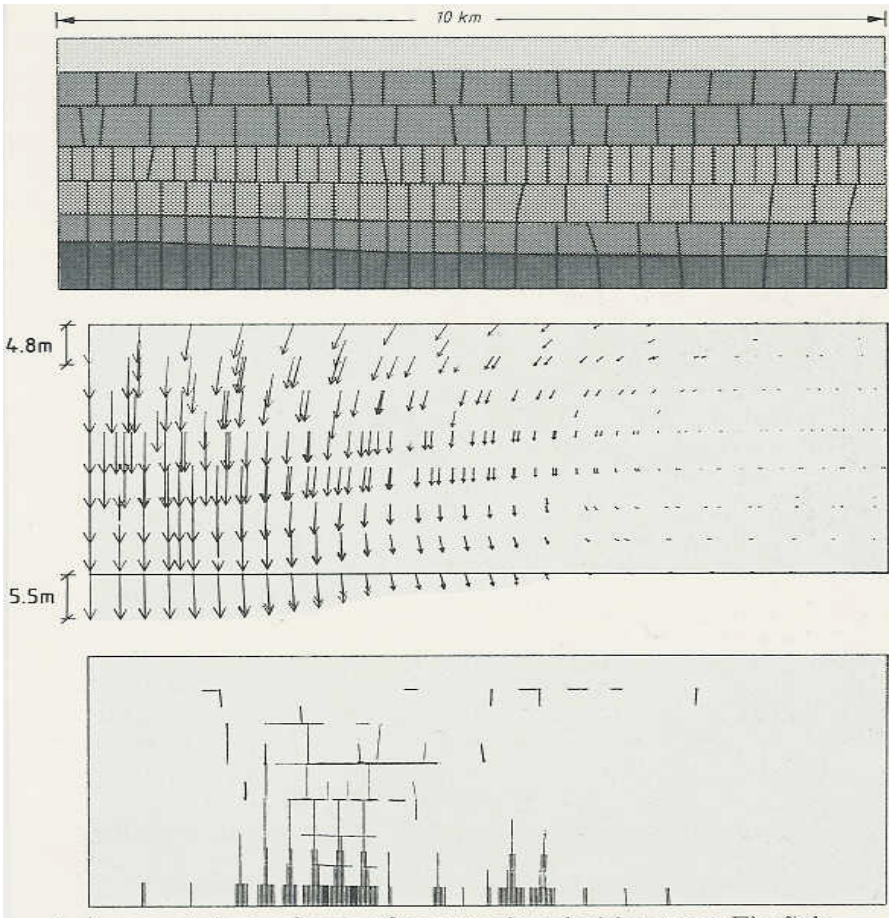

Figure 18. Two-dimensional, axi-symmetric modelling of a compaction-subsidence increment of the Ekofisk reservoir and over-burden. Barton et al., 1988.The inevitable simplification of an assumed bedded/faulted/jointed over-burden nevertheless shows inter-bed shear and intra-bed opening, due to the stretch caused by the subsidence. Such 'structural' mechanisms could readily explain shear-wave polarization 'squareness' in a shallow over-burden, as in Figure 17.

THE ROLE OF COMPLIANCES

Shear-wave anisotropy due to splitting and polarization caused by the presence of vertical or aligned structure, and P-wave azimuthal anisotropy, are miraculous means for rectifying the poor core-sampling strategy of mostly vertical exploration holes, in view of the long seismic wave lengths. The presence of the fracture sets clearly affects the elastic moduli of the fractured rock mass, due to the addition of their dynamic compliances. The additional presence of the fractures is expressed as the sum of the compliance of the isotropic back-ground rock and the *excess compliance* matrix associated with the fractures. The latter is composed of the effects of a fracture normal compliance Z_N, and a fracture shear compliance Z_T. These are likely to be effective stress-dependent, and there may be two sets to contend with.

Involvement of normal compliance (Z_N) in the slow shear wave velocity that helps to detect oil or gas, due to fluid compressibility differences (e.g. Van der Kolk et al. 2001, and Sayers, 2002), actually requires dipping fractures, or non-vertical wave propagation. When polarized shear-waves sense the different compressibility of oil or gas in the fractures, Z_N would seem more likely to be involved than Z_T, which would have a less obvious dependence on fluid compressibility differences.

Shear compliance, as opposed to *normal* compliance is of most relevance in the case of vertical shear-waves and vertical structure, and the resulting degree of shear-wave anisotropy. The degree to which dynamic *shear compliances* might be related, more weakly than in the pseudo-static case (Barton et al., 1985), but nevertheless directly to *block size*, is a remaining unsolved problem in this important area of seismic detection of anisotropy, and is an important goal for improved interpretation of anisotropic reservoir permeability, and its temporal variation in 4D time-lapse studies.

Despite some earlier literature claiming possible near-equality of the two compliances, possibly partly based on some physical modelling of less representative Perspex-plate laminates, an *inequality* of the joint or fracture compliances Z_N and Z_T would be more consistent. There is a large body of experience of $K_s < K_n$, concerning the *pseudo-static* shear and normal *stiffnesses* of joints and fractures, where stiffness is the rough inverse of compliance (Barton, 1986, 2006). Dynamic compliances, miraculously, have the same (but inverted) units as pseudo-static (i.e. larger displacement) stiffness testing of rock joints. The magnitude of K_n proves to be less than, but quite close to $1/Z_N$, while in the shearing direction, $K_s < 1/Z_T$ *perhaps* $<< 1/Z_T$. However Z_T data are extremely limited in geophysics, compared to the large body of K_s (pseudo-static) lab and field data, from the sometimes less complicated field of rock mechanics.

A handful of dynamic loading tests on 50 mm size laboratory samples of natural joints, (Pyrak-Nolte et al. 1990), on 40 mm size induced tension fractures (King, 2002), and on 50 mm diameter artificial fractures, and occasional cross-hole seismic testing in quarries (Lubbe, 2005, Lubbe and Worthington, 2006), unfortunately represent an uncertain basis for interpreting the degree of inequality $Z_N \leq Z_T$ and their likely magnitudes for *fractured reservoirs* with oil or gas saturation.

Convenient 'core-sized' 50 mm joint samples from hard crystalline rock (quartz monzonite from the Stripa mine in Sweden), subject to state-of-the-art testing by Pyrak-Nolte et al. 1990, are logically-speaking and unfortunately, *unlikely* to have 1:1 relevance to *in situ* reservoirs in mostly much weaker

sedimentary rock, where jointed block sizes may also range from extremes of perhaps 100 mm to 10,000 mm. Depending on stress levels, on rock wall strength (described by JCS), and on wall roughness (described by JRC), the dynamic normal stiffness $K_{n(dyn)}$ may range from 10^{12} to 10^{14} Pa/m, or 1,000 to 100,000 MPa/mm (also 1 to 100 MPa/μm), suggesting a mostly very small increment of dynamic displacement.

By comparison, $K_{n(static)}$ values from a wide range of weaker rock and joint types, may vary from as low as 100 MPa/mm at low stress, to almost 50,000 MPa/mm at equivalent high stress. There is therefore a large degree of overlap between the static and dynamic stiffnesses in this *stiffest* normal-loading direction (Barton, 2006).

CONCLUSIONS

1. The geophysics literature concerned with shear-wave polarization is largely focussed on an assumed line-up of 'open' features and the maximum horizontal stress $\sigma_{H\ max}$, whether these are micro-cracks or reservoir macro-fractures.

2. Geomechanics modelling using the Barton-Bandis roughness JRC and wall strength JCS parameters, suggests that 'open' joints or fractures that are acted on by tens of MPa normal stress, consisting of $\sigma_{H\ min}$ at several kilometer reservoir depths, will need to be rough-surfaced and of relatively high strength for them to be considered 'open', unless mineral bridging and channel flow are involved.

3. Water-flow and fracture-orientation logging in deep wells in crystalline rock of generally higher strength than reservoir rocks, as performed on many occasions by University of Stanford researchers since 1995, suggest that for fractures to have permeability at many kilometres depth, they need to be under shear stress. They are then more likely to be conjugate sets bisected by $\sigma_{H\ max}$. The fractures parallel to $\sigma_{H\ max}$ at many kilometres depth tend to be non-conducting, and therefore not 'open' as generally assumed in geophysics literature.

4. Both P-wave AVO studies and shear-wave polarization studies reported in the literature contain a number of examples of 'deviation' between major stress and 'openness', or between the major stress and the fast shear-wave direction, or between the axis of minimum attenuation and the major stress direction. It is suggested that these cases are caused by two unequal sets of fractures that may be contributing their unequal compliances and fracture frequencies, and that are roughly bisected by $\sigma_{H\ max}$. If permeable and acted on by shear stress they would also be consistent with geomechanics logic.

5. Rosettes showing the fast shear-wave axes from shear-wave polarization interpretation of numerous earthquakes from many countries, present familiar symmetries that suggest tectonic features aligned with, or bisected by, major horizontal stress, rather than stress-aligned microcracks alone.

6. Production from domal or anticlinal reservoir structures, with dipping conjugate sets of fractures, can be shown by geomechanics modelling of the compaction process to cause unequal down-dip shearing on the fracture sets, in addition to the contraction of the high porosity matrix.

7. Newly developed slickensides identified many years after exploration are evidence for such a mechanism at Ekofisk, and were discretely modelled prior to recognition of this production-related slickensiding. Such mechanisms can be responsible for temporal rotation of anisotropy and attenuation axes identified in 4D monitoring, if unequally sheared fracture sets with unequal strike are present in the reservoir.

8. Over-burden stretch causing unequal apertures as one rotates around a subsidence bowl, are logically caused by intra-bed jointing. The 'squareness' of the qS_1 directions, and the relative magnitudes of the time-delay length scales, show a logical match to regions of smaller and larger bending of the subsiding over-burden strata.

9. The normal and shear compliances of fractures are unlikely to be of equal magnitude, since they are fundamentally different deformation mechanisms. Laboratory tests of 40 and 50 mm joint and fracture samples are unlikely to be applicable to generally much larger in situ reservoir block sizes. The dynamic compliances Z_N and Z_T are described by the same, but inverted units of stiffness as those obtained in pseudo-static large-deformation testing of Kn and Ks in rock mechanics. The 'common' rock mechanics units (MPa/mm), or the geophysicist inverse ($m.Pa^{-1}$), suggest that friction is a valid attenuation mechanism, however small the displacement discontinuity.

REFERENCES

Albright, J., Dangerfield, J., Johnstad, S., Cassell, B., Deflandre, J-P., & R. Withers, 1994. Seismic Surveillance for Monitoring Reservoir Changes. *Oilfield Review, January, 1994,* Schlumberger.

Bakulin, A., Grechka, V. & I. Tsvankin, 2001. Estimation of Fracture Parameters of Monoclinic Media from Reflection Seismic Data. *9th IWSA (Int. Workshop on Seismic Anisotropy), Abstracts, Geophysics, 66:* 4, 1294-1312.

Barkved, O., Bartman, B., Gaiser, J., Van Dok, R., Johns, T., Kristiansen, P., Probert, T. & Thompson, M. 2004. The Many Facets of Multicomponent Seismic Data. *Oilfield Review, Summer 2004*, 42-56.

Barton, C.A., Zoback, M.D. and Moos, D. 1995. In situ stress and permeability in fractured and faulted crystalline rock. *Mechanics of Jointed and Faulted Rock.* Rossmanith (ed.) 381-396. Balkema, Rotterdam.

Barton, N. 1973. Review of a new shear strength criterion for rock joints. *Engineering Geology*, Elsevier, Amsterdam, Vol. 7, 287-332. Also NGI Publ. 105, 1974.

Barton, N., Bandis, S. & Bakhtar, K. 1985. Strength, deformation and conductivity coupling of rock joints. *Int. J. Rock Mech. & Min. Sci. & Geomech. Abstr. 22:3:* 121-140.

Barton, N., Hårvik, L., Christiansson, M., Bandis, S., Makurat, Chryssanthakis, P. & Vik, G. 1986. Rock mechanics modelling of the Ekofisk reservoir subsidence.*Proc. 27th US Rock Mech. Symp*., Univ. of Alabama.

Barton, N., Makurat, A., Hårvik, L., Vik, G., Bandis, S., Christianson, M. & Addis, A. 1988. The discontinuum approach to compaction and subsidence modelling as applied to Ekofisk. BOSS '88. Proc. of Int. Conf. on Behaviour of Offshore Structures, Trondheim. Vol. 1: 129-141.

Barton, N. 1986. Deformation phenomena in jointed rock. 8th Laurits Bjerrum Memorial Lecture, Oslo. Geotechnique, Vol. 36: 2: 147-167.

Barton, N. 2006. Rock Quality, Seismic Velocity, Attenuation and Anisotropy. Taylor & Francis, UK and Netherlands, 729 p.

Boness, N.L. & Zoback, M.D. 2006. A multiscale study of the mechanisms controlling shear velocity anisotropy in the San Andreas Fault Observatory at Depth. *Geophysics,* 71, 5, F131-F146.

Crampin, S. & Lovell, J.H. 1991. A decade of shear-wave splitting in the Earth's crust: What does it mean? What use can be made of it? And what should we do next? *Geophys. J. Int., 107:* 387-407.

Crampin, S. & D.C. Booth, 1989. Shear-wave splitting showing hydraulic dilation of pre-existing joints in granite. *Scientific Drilling,* 1, 21-26.

Gao, Y., Wu, J., Chen, Y-T., Huang, J-L. & Shi, Y-T. 2006. Crustal seismic anisotropy in capital area of China and its tectonic implication. *Proc. of 12th International Workshop on Seismic Anisotropy,* Beijing.

Gaiser, J. & van Dok, R. 2003. Converted Shear-Wave Anisotropy: New Technology for Fractured-Reservoir Management. *AAPG Int. Conf., Barcelona, Spain.*

Heffer, K. 2002. Geomechanical influences in water injection projects: An overview. *Oil & Gas Science & Technology – Rev. IFP, 57:5:* 415-422.

King, M.S. 2002. Elastic wave propagation in and permeability for rocks with multiple parallel fractures. Technical Note*, Int. J. Rock Mech. & Min. Sci., 39:* 1033-1043.

Laubach, S., Gale, J.F.W. & Olson, J.E. 2002. Are Open Fractures Necessarily Aligned with Maximum Horizontal Stress? *American Assoc. of Petr. Geologists. (AAPG: Fractured Reservoirs and Multi-Phase Fluid Flow),* Annual Meeting, Houston, Texas.

Laubach, S., Marrett, R. & Olson, J. 2000. New directions in fracture characterization. *The Leading Edge,* July 2000, 704-711.

Liu, E., Crampin, S., Queen, J.H. & Rizer, W.D. 1993. Velocity and attenuation anisotropy caused by microcracks and macrofractures in a multiazimuth reverse VSP. *Canadian J. Expl. Geophy., 29:* 177-188.

Lubbe, R. 2005. A field and laboratory investigation of the compliance of fractured rock. *D.Phil. Thesis,* Oxford University.

Lubbe, R. & Worthington, M.H. 2006. A field investigation of fracture compliance. *Geophys. J. Int.,* 155, 1, 221-240.

Maultzsch, S., M. Chapman, E. Liu and X-Y. Li, 2005. Observation and modelling of anisotropic attenuation in VSP data. Seismic Q – Observation, Mechanisms, and Interpretation: *Workshop at 67th EAGE Conference, Madrid.* Extended Abstract, Q-08, Convenors: Hargreaves, Best and Lancaster.

Olofsson, B. & Kommedal, J. 2002. Facing the processing challenges of the Valhall 1998 3D 4C OBS data. Extended Abstract: Geophysics in a shared earth model. *Symposium, Norwegian Petroleum Society NPF, Kristiansand,* 103-106.

Pérez M.A., Grechka, V. & Michelena, R.J. 1999. Fracture detection in a carbonate reservoir using a variety of seismic methods. *Geophysics, 64:4:* 1266-1276.

Pyrak-Nolte, L.J., Myer, L.R. & Cook, N.G.W. 1990. Transmission of seismic waves across single natural fractures. *J. Geophys. Res., 95:* 8617-8638.

Queen, J.H. & Rizer, W.D. 1990. An Integrated Study of Seismic Anisotropy and the Natural Fracture System at the Conoco Borehole Test Facility, Kay County, Oklahoma. *J. Geophys. Res., 95:B7:* 11,255-11,273.

Smith, R.L. & McGarrity, J.P. 2001. Cracking the fractures – seismic anisotropy in an offshore reservoir. *The Leading Edge*, Jan. 18-26.

Sayers, C.M. 2002. Fluid-dependent shear-wave splitting in fractured media. *Geophys. Prospect., 50:* 393-401.

Stenin, V.P., Kasimov, A.N. & Tikhonov, A.A. 2002. Cracked layers characterization using far offset VSP. 10th International Workshop on Seismic Anisotropy.

Tingay, M., Müller, B., Reinecker, J., Heidbach, O., Wenzel, F. & Fleckenstein, P. 2005. Understanding tectonic stress in the oil patch: The World Stress Map Project. The Leading Edge, Dec. 2005, 1276-1282.

Townend, J. and Zoback, M.D. 2000. How faulting keeps the crust strong. *Geology,* 28, 5: 399-402.

Zoback, M.D. & Townend, J. 2001. Implications of hydrostatic pore pressures and high crustal strength for the deformation of intraplate lithosphere. *Tectonophysics, 336:* 19-30.

Van der Kolk, C.M., Guset, W.S. & Potters, J.H.H.M. 2001. The 3D shear experiment over the Naith field in Oman: the effect of fracture-filling fluids on shear propagation. *Geophys. Prospect.*, *49:* 179-197.

Wu, J., Gao, Y., Cai, J., Shi, Y., Lin, S., Bao, T. & Li, Z. 2006. Seismic anisotropy in the crust in Fujian area, southern China. *Proc. of 12th International Workshop on SeismicAnisotropy,* Beijing.